Carbohydrate Polymers 86 (2011) 120–126

Contents lists available at ScienceDirect

Carbohydrate Polymers

journal homepage: www.elsevier.com/locate/carbpol

Self-assembly of carboxymethyl konjac glucomannan-*g*-poly(ethylene glycol) and (α-cyclodextrin) to biocompatible hollow nanospheres for glucose oxidase encapsulation

Quan Li[a], Bing Xia[a], Mickey Branham[c], Wei Ha[a], Hao Wu[a], Shu-Lin Peng[a], Li-Sheng Ding[a], Bang-Jing Li[a,*], Sheng Zhang[b,**]

[a] Key Laboratory of Mountain Ecological Restoration and Bioresource Utilization, Chengdu Institute of Biology, Chinese Academy of Sciences, Chengdu, Sichuan 610041, PR China
[b] State Key Laboratory of Polymer Materials Engineering (Sichuan University), Polymer Research Institute of Sichuan University, Chengdu, Sichuan 610065, PR China
[c] School of Pharmacy and Pharmacology, University of KwaZulu-Natal, Durban 4000, South Africa

ARTICLE INFO

Article history:
Received 16 February 2011
Received in revised form 7 April 2011
Accepted 10 April 2011
Available online 15 April 2011

Keywords:
Biocompatibility
Carboxymethyl konjac glucomannan
Enzyme encapsulation
Nanospheres
Self-assembly

ABSTRACT

The self-assembly of rod–coil carboxymethyl konjac glucomannan-graft-poly(ethylene glycol) (CKGM-*g*-PEG) and α-cyclodextrin (α-CD) complexes were investigated and used as encapsulating hollow nanospheres for the enzyme glucose oxidase (GOX) in aqueous solution. These hollow nanospheres exhibited "cell-like" semi-permeability allowing enzyme substrates to pass through the surface while restricting the encapsulated enzyme (i.e. GOX) to the interior. Encapsulated GOX exhibited higher thermostability, optimal enzymatic activity over a wider pH range and improved storage stability in comparison to free un-encapsulated GOX. In addition, these CKGM-*g*-PEG/α-CD hollow nanospheres showed in vitro biocompatibility when exposed to L929 cells when tested using MTT viability assay. These studies suggested that self-assembly of CKGM-*g*-PEG and α-CD to form stable nanospheres may be an effective method for enzyme encapsulation with numerous biomedical applications.

1. Introduction

Konjac glucomannan (KGM) is a high molecular weight, water-soluble polysaccharide composed of (1 → 4) linked D-glucose and D-mannose units in the molar ratio 1:1.6 to 1:1.69. It is isolated from the tubers of the species *Amorphophallus. konjac*, a major crop found in the mountain areas of China and Japan. KGM has been used traditionally as a prophylactic remedy against diabetes and heart disease (Chen, Cheng, Liu, Liu, & Wu, 2006; Li, Xia, Wang, & Xie, 2005). Carboxymethylation of KGM produces an anionic polymer (CKGM) that has good water solubility and excellent gelation properties when mixed with a polymer of opposite charge. Because of these properties, its bioactivity and biocompatibility (Wu & Chen, 2008), CKGM is considerd as a promising biomaterial for pharmaceutical development (Du et al., 2004; Nakano, Takikawa, & Arita, 1979; Wang & He, 2002) and enzyme encapsulation. While, large-scale applications of CKGM are still rare, drug delivery and enzyme encapsulation vehicles made from CKGM have been prepared via polyelectrolyte complexation. For instance, our group recently reported a novel form of nanocapsules made from CKGM–chitosan for L-asparaginase encapsulation (Wang et al., 2008).

Polymeric hollow spheres may be ideal structures for the encapsulation of large quantities of guest molecules or for large-sized guests within the core domain of the polymer (Du & O'Reilly, 2009). Activity in this area of research has increased since rigid–coil copolymer self-assembly and the direct formation of hollow spheres in a selective solvent were described (Jenekhe & Chen, 1998, 1999). This novel approach has aroused recent investigations in our group and other using rigid/coil systems to construct hollow spheres. Several reports have demonstrated the use of hydrogen-bonding interactions between rod-like and coil-like polymers which directly self-assemble into hollow spheres (Chen & Jiang, 2005; Duan et al., 2001; Duan, Kuang, Wang, Chen, & Jiang, 2004). These self-assembled hollow spheres, however, lack biocompatibility and biodegradability because the rod-like blocks were formed by synthetic methods. For biomedical and drug delivery applications however, self-assembly and the formation of hollow nanospheres that are biocompatible and non-toxic would be most desirable.

Recently, we developed a novel approach to prepare rod–coil complexes by self-assembly using alginate-*g*-poly(ethylene glycol) and α-CD (Meng et al., 2010). These complexes did effectively self-assemble into hollow spheres and showed good encapsulation

* Corresponding author. Tel.: +86 28 85228831; fax: +86 28 85222384.
** Corresponding author. Tel.: +86 28 85400266; fax: +86 28 85400266.
E-mail addresses: libj@cib.ac.cn (B.-J. Li), zslbj@163.com (S. Zhang).

0144-8617/$ – see front matter © 2011 Elsevier Ltd. All rights reserved.
doi:10.1016/j.carbpol.2011.04.017

behavior of L-asparaginase in aqueous solution (Ha et al., 2010). Based upon these previous results we have prepared biocompatible CKGM-*g*-PEG/α-CD hollow nanospheres for glucose oxidase (GOX) encapsulation and characterization.

GOX is a flavin containing dimeric glycoprotein (160 kDa) with numerous potential applications in biosensor, bioreactor and drug delivery technology (Lin, Lu, Tu, & Ren, 2004; Napoli et al., 2004; Qiu & Park, 2001). Several methods of GOX encapsulation with the aim to enhance or preserve enzyme activity have been described (Pandey et al., 2007; Taylor, 1991; Trau & Renneberg, 2003; Zhu, Srivastava, Brown, & McShane, 2005), but to the best of our knowledge, GOX encapsulation in hollow nanospheres prepared by the rod–coil self-assembly method has not been reported.

In this paper we describe the preparation, structural and biocatalytic properties of GOX-encapsulated CKGM-*g*-PEG/α-CD hollow spheres. The percentage of enzyme encapsulation and leakage efficiency is also studied. Enzyme activity and stability under different temperatures and pH conditions were carried out to evaluate the difference between the free and encapsulated enzyme. Use and potential applications of these CKGM-*g*-PEG/α-CD hollow spheres in various fields are discussed.

2. Materials and methods

2.1. Materials

KGM was purchased from Chengdu Root Industry Co., Ltd. (Chengdu, China). Methoxy poly(ethylene glycol) (mPEG, Mn = 2000), N-tert-butoxycarbonylglycine (N-t-Boc-glycine), 4-(dimethylamino) pyridine (DMAP), 1-ethyl-3-[3-(dimethylamino)propyl]-carbodiimide (EDC), dicyclohexylcarbodiimide (DCC), morpholinoethane sulfonic acid (MES), N-hydroxysuccinimide (NHS) and trifluoroacetic acid (TFA) were procured from Sigma Aldrich (Shanghai, China). α-CD was purchased from Tokyo Chemical Industry Co., Ltd. (Japan). CKGM was prepared as described by Shinsaku et al. (Kabayashi, Tsujihata, Hibi, & Tsukamoto, 2002). The degree of substitution was found to be 63.7% measured according to methods described in the literature (Smith, 1967). Glucose oxidase (50 U/mg) was purchased from Aladdin Reagent Co., Ltd. (Shanghai, China) and prepared as a 1 mg/mL solution. All other reagents were of analytical grade and were used directly without further purification. All solvents and water were redistilled before use.

2.2. Preparation and characterization of CKGM-g-PEG

CKGM-*g*-PEG was prepared using four [mPEG/CKGM] molar ratios (i.e. CP200 [2.0], CP180 [1.8], CP140 [1.4] and CP100 [1.0]) by our previously described method (Xia et al., 2010). The typical procedure is illustrated for CP200: CKGM 2.5 g is dissolved in 100 mL of a solution containing 0.1 M MES buffer and 0.5 M NaCl. The pH was adjusted to 6.0 with HCl or NaOH after complete mixing. Crosslinking reagents EDC and NHS (molar ratio of EDC:NHS:COO^- = 1:0.5:1) were then added to the CKGM solution. The solution was stirred continuously while adding 6.0% (w/v) mPEG–$OCOCH_2NH_2$ in MES buffer solution, which was then allowed to reaction at room temperature for 10 h. The resulting mixture was dialyzed against pure water for 48 h and dried under vacuum. The dried product removed was then washed 3 times with 5 mL acetone and 5 mL chloroform to remove residual mPEG and the organic reagents. The washed product was then dried under vacuum at room temperature until characterized by ^{1}HNMR or TGA.

Proton NMR spectra were recorded in D_2O using a 600 MHz spectrometer (Avance Bruker-600, Switzerland). The degree of mPEG substitution (DS) to CKGM as a measure of graft mass-transition was calculated according to thermal gravimetric analysis (TGA). A TA Q500 thermo analyser (TA instruments, Delaware, USA) was used at the heating rate of 10 °C/min under N_2 atmosphere in the temperature range of 25–500 °C. The DS was calculated using the following Eqs. (1) and (2), where 2000 is the number average molecular weight of mPEG, and 212.9 is the molar mass of a CKGM unit.

$$\text{Percentage of CKGM component in CP (\%)} = \frac{\text{CKGM component weight loss} + \text{sample residue}}{1 - \text{water weight loss}} \times 100 \quad (1)$$

$$\text{DS (\%)} = \frac{212.9 \times (1 - \text{percentage of CKGM component in CP})}{2000 \times \text{percentage of CKGM component in CP}} \times 100 \quad (2)$$

2.3. Preparation of the hollow nanospheres and GOX encapsulation procedure

CKGM-*g*-PEG solutions (1 mL acetate buffer, pH = 6.5) in the concentration range (0.1–0.5%, w/v) were prepared for enzyme encapsulation studies. GOX (0.5 mg) was then added to the CKGM-*g*-PEG solutions and mixed continuously before dropwise addition to the α-CD acetate buffer solution (2.5 mL, 6% (w/v), pH = 6.5) while stirring at 10 °C. After continuous stirring for 1 h, the hollow nanospheres were collected by centrifugation at 13,000 rpm for 10 min (TGL-20M, Saite Centrifuge Co., Shanghai, China). The supernatant liquids were then collected for determination of GOX encapsulation efficiency via UV absorbance (see Section 2.6).

2.4. Characterization of the hollow nanospheres

The size of the nanospheres was measured by dynamic light scattering (DLS; BI-9000AT, BI-200SM, Brookhaven Instruments Co., USA) in aqueous solution at 25 °C, wavelength 532 nm, and detection angle of 90°. Each sample was measured three times with the results represented as the mean diameter for two replicate samples. Transmission electron microscopy (TEM) was performed on a JEOL JEM-100CX instrument operating at an accelerating voltage of 80 kV. Samples were placed onto a copper grid, dried at room temperature, then examined without prior staining. Atomic force microscopy (AFM) images were obtained in tapping mode with a Nanoscope IIIa Digital Instrument. Mica was used as substrate for the sample preparation. Crystalline structures of the hollow nanospheres were characterized by X-ray powder diffraction, performed using Cu-K alpha irradiation source with X'Pert MPD (20 kV; 35 mA; 2° theta/min).

2.5. In vitro biocompatibility test of nanospheres

Nanosphere biocompatibility was evaluated against L929 cells by methyl tetrazolium (MTT) assay in a 96-well plate format. Cells were cultured in 96-well culture plates at a density of 1×10^4 cells per well in Dulbecco's modified Eagle's medium (DMEM, GIBCO BRL, USA) supplemented with 10% fetal bovine serum (National HyClone Bio-Engineering Co., Ltd., Lanzhou, China) at 37 °C in a humidified environment of 5% CO_2 for 24 h. The cells were then exposed to nanospheres extracted with culture medium and incubated for another 24 h at 37 °C in the humidified environment of 5% CO_2. Polystyrene and 0.5% phenol were used as negative and positive controls, respectively. After 24 h, the wells in one plate were replenished with 100 μL DMEM containing 10% fetal bovine serum. Then 50 μL of 1 mg/mL MTT solution was added to each well and incubated for another 2 h. The MTT solution was then replaced

with 100 μL isopropanol and the plate shaked for 1 min to produce a homogeneously coloured solution. Optical absorbance was then read at wavelength 570 nm (650 nm reference) on a Bio-rad 550 Microplate Reader. The cell growth (RCG %) relative to control cells containing cell culture medium without nanospheres was calculated from Eq. (3):

$$\mathrm{RCG}\,(\%) = \frac{[\mathrm{OD}]\mathrm{text}}{[\mathrm{OD}]\mathrm{control}} \times 100 \quad (3)$$

2.6. Determination of GOX encapsulation efficiency and leakage efficiency

In order to determine the encapsulation efficiency of the nanospheres, it is necessary to detect the free enzyme in the supernatant. Free and encapsulated GOXs were separated by centrifugation of the suspension at 13,000 rpm for 10 min. The supernatant was diluted to 5.0 mL and then assayed by UV spectrophotometry. The GOX encapsulation efficiency was calculated using Eq. (4):

$$\text{Encapsulation effciency}\ (\%) = \frac{\text{mass of GOX used in formulation} - \text{mass of free GOX}}{\text{mass of GOX used in formulation}} \times 100 \quad (4)$$

To evaluate diffusion or leakage of GOX out of the hollow nanospheres, samples of the hollow nanospheres containing GOX were stored in 2 mL acetate buffer (pH 6.5) at 4 °C for 48 h. This mixture was again separated by centrifugation at 13,000 rpm for 10 min and the clear supernatant was collected for determination of GOX leakage efficiency using the following equation (5):

$$\text{Leakage efficiency}\ (\%) = \frac{\text{mass of GOX in the supernatant}}{\text{mass of GOX encapsulated}} \times 100 \quad (5)$$

Total protein concentration in each sample was also assessed by the Bradford method (Bradford, 1976).

2.7. Determination of encapsulated vs. free GOX activity

The indigo carmine method (Dai, Li, & Jiang, 1998; Li, Du, Boullanger, & Jiang, 1999; Zhou, Chen, & Wang, 2008) was used to study the enzymatic activity of GOX after encapsulation in hollow nanospheres. Briefly, a 0.2 M glucose solution was used as substrate. After GOX catalyzed conversion of β-D-glucose to D-gluconic acid, the released H_2O_2 oxidizes the indigo dye to effect change in absorbance. Optical absorbance of the solution at 615 nm was monitored spectrophotometrically (APL-UV-2000, Shanghai, China) and the absolute activities of the encapsulated and free enzyme were calculated according to the standard curve. In these experiments the activity unit (U) of GOX is defined as the amount of enzyme required to produce 1 μg hydrogen peroxide per minute at 37 °C.

2.8. Turbidity experiment

Brief procedures: 0.5 mg GOX was mixed with each of the following solutions, (a) 4 mL 6% α-CD solutions, (b) 4 mL 0.2% CKGM-*g*-PEG solutions, and (c) 4 mL mixture of 6% α-CD plus 0.2% CKGM-*g*-PEG solutions. The absorbance of each solution at 615 nm was recorded with a UV spectrophotometer (APL-UV-2000, Shanghai, China).

Table 1
The degree of PEG substitution (DS) of CKGM-*g*-PEGs and the mean diameter of the nanospheres.

Sample	DS of CKGM-*g*-PEG (mol%)	Mean diameter[a] (nm)
CP200/α-CD	54.9	402 ± 50
CP180/α-CD	34.6	1016 ± 33
CP140/α-CD	27.6	1165 ± 152
CP100/α-CD	18.7	1157 ± 112

[a] The nanospheres were formed by 0.2% CP and 6.0% α-CD.

3. Results and discussion

3.1. Characterization of CKGM-g-PEG

The formation of CKGM-*g*-PEG is evidenced by ^{1}H NMR (CP200 is shown as an example in Fig. S1). The strong –CH_2– peaks of PEG are present between 3.50 and 3.80 ppm. The methoxy group of mPEG appears at about 3.30 ppm. The signal at 4.30 ppm demonstrates the existence of terminated –CH_2– linked to the glycine segment of mPEG. The peak at 4.19 ppm is assigned to –CH_2– of the glycine segment, but before the formation of CKGM-*g*-PEG, this signal was located at 3.91 ppm, which further confirms the connection of CKGM and PEG (Xia et al., 2010).

The TGA thermograms of CKGM-*g*-PEG copolymers are shown in Fig. S2. These grafted copolymers displayed three main stages of degradation, to include (1) a moisture loss at a temperature 100 °C, followed by (2) a major weight loss of the CKGM component at about 270 °C and (3) another subsequent weight loss of the PEG component around 370 °C. Since the decomposition temperature interval of the CKGM component and the PEG component is significant, the degree of PEG substitution (DS) can be calculated using Eqs. (1) and (2) with the results summarized in Table 1. Degree of substitution apparently increases with increasing [mPEG/CKGM] molar ratios.

3.2. Preparation of CKGM-g-PEG/α-CD hollow spheres for GOX encapsulation

CKGM-*g*-PEGs are water-soluble copolymers, which form transparent solutions in water. When aqueous solutions of α-CD were added to solutions of CKGM-*g*-PEG at room temperature, gradual increases in turbidity were observed (Fig. 1), that normally indicates aggregate formation. This observation is consistent with previous reports of PEG/α-CD inclusion complex formation in water wherein the resulting rod-like crystallites are water-insoluble because the α-CD molecules are able to pack more closely through hydrogen bonding (Ceccato, Nostro, & Baglioni, 1997). Fig. 2 shows the X-ray diffraction (XRD) patterns of the α-CD (a), PEG/α-CD inclusion complex (b), CKGM-*g*-PEG/α-CD (c), and CKGM-*g*-PEG

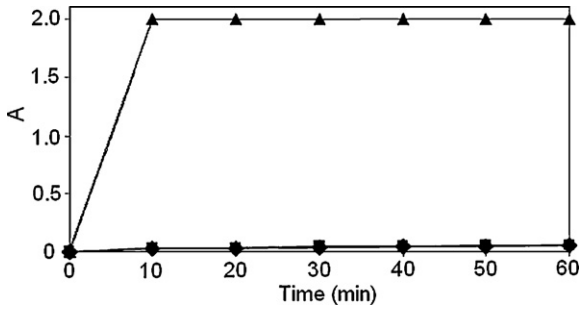

Fig. 1. Turbidity plot at λ = 615 nm (the mixture of α-CD and enzyme, inverse squares; the mixture of CKGM-*g*-PEG and enzyme, squares; the mixture of CKGM-*g*-PEG, α-CD and enzyme, triangles).

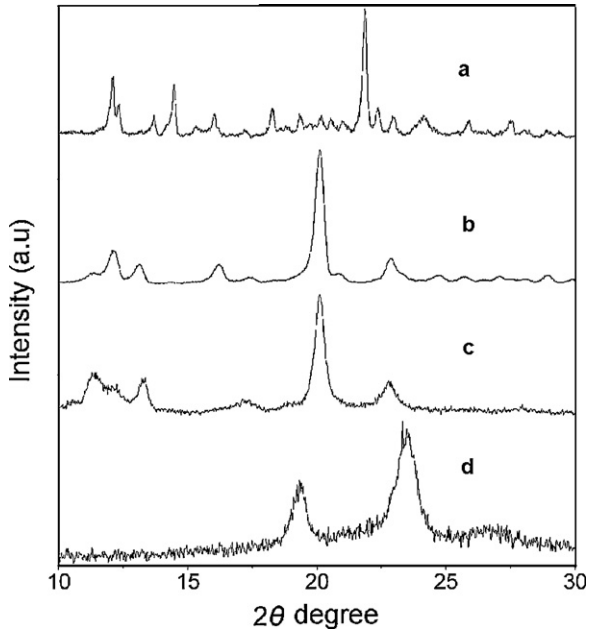

Fig. 2. X-ray diffraction patterns of (a) α-CD, (b) PEG/α-CD inclusion complex, (c) CKGM-*g*-PEG/α-CD particles, (d) CKGM-*g*-PEG.

(d). It can be seen that the pattern of CKGM-*g*-PEG/α-CD differs from that of free CKGM-*g*-PEG or α-CD. The homoPEG crystalline peaks (2 theta = 19.2° and 23.3°) and α-CD crystalline peak (2 theta = 21.5°) were absent. The peak at 2 theta = 19.9° is a typical peak of PEG-α-CD channel-type crystallites (Harada & Kamachi, 1990; Harada, Li, & Kamachi, 1993) indicating that CKGM-*g*-PEG/α-CD contained PEG-α-CD inclusion structures. During the formation of insoluble PEG-α-CD inclusion blocks, water becomes a selective solvent for the CKGM-*g*-PEG/α-CD, so that micelle-like aggregates were formed. The expected structure of CKGM-*g*-PEG/α-CD in aqueous solution is an inner rod-like PEG-α-CD inclusion block surrounded by a protonated coil-like CKGM shell. Jenekhe et al. and Jiang et al. have confirmed that this rod-like block in rod–coil system preferred parallel packing which may result in the formation of hollow spheres promoted by efficient space-filling (Chen & Jiang, 2005; Duan et al., 2001; Duan, Kuang, Wang, Chen, & Jiang, 2004; Jenekhe & Chen, 1998, 1999).

Turbidity experiments indicated no increases in light-scattering intensity when GOX was mixed with CKGM-*g*-PEG or α-CD solutions (Fig. 1), this suggests that GOX does not form aggregates with CKGM-*g*-PEG or α-CD molecules. After addition of GOX to the solution during the process of self-assembly of CKGM-*g*-PEG and α-CD, and then separated by centrifugation, the amount of GOX in the supernatant decreased significantly, again indicating entrapment of the enzyme within the CKGM-*g*-PEG/α-CD aggregates. The encapsulation procedure can be illustrated schematically in Fig. 3.

3.3. Morphology and sizes of the nanospheres

Aggregate morphology was studied by TEM and AFM. As shown in Fig. 4a, the outer shell and central core of the particles are easily distinguished; a typical TEM image of hollow sphere which appear like those reported for other types of hollow particles (Caroso, Caroso, & Möhwald, 1998; Xu & Asher, 2004).

After GOX encapsulation, bright domains could not be found in these particles and the cores were slightly darker than the outlines of spheres. The micrographs indicating that the hollow spheres filled with the enzyme restricted them to the inner space (Fig. 4b). Similar conclusions were derived from the AFM experiments which determined different heights between un-loaded and enzyme-loading spheres (Luo et al., 2010). In the AFM micrographs, CKGM-*g*-PEG/α-CD nanospheres without GOX also showed rounded line shapes, but it should be noted that the height of the aggregates (10 nm) (Fig. 4c), was about 30 times smaller than the average diameter of horizontal direction. Such remarkable size differences between the horizontal and vertical direction of spheres may be due to collapsing of the hollow spheres (Luo et al., 2010). However, after the enzyme encapsulation, the height of aggregates increased to approximately 57 nm (Fig. 4d), about 5-fold increase in the height of hollow spheres without GOX. Increase of aggregates height further demonstrated that the GOX has been encapsulated into the CKGM-*g*-PEG/α-CD hollow spheres instead of merely associated with its exterior. The AFM or TEM measured diameters of the spheres in Fig. 4 is a bit smaller than that from DLS testing, which maybe due to the shrinkage of particles during the process of the solvent evaporation in sample preparation (Ha et al., 2010).

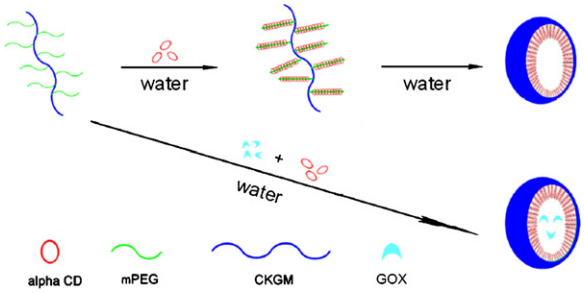

Fig. 3. Construction of hollow nanospheres and the process of enzyme encapsulation.

Particle sizes of the hollow spheres were also evaluated by DLS and the results are displayed in Table 1. When the DS of PEG decreased from 54.9% to 27.6%, the mean diameter of the nanoparticles increased from approximately 400 nm to 1100 nm. This trend of the size varying with "graft density" is consistent with that reported for the other rod–coil complexes (Chen & Jiang, 2005; Duan et al., 2001; Duan, Kuang, Wang, Chen, & Jiang, 2004; Meng et al., 2010). But it should be noted that when the DS of PEG decreased further (from 27.6% to 18.7%), the sizes of the particles did not change significantly.

3.4. Encapsulation efficiency of the CKGM-*g*-PEG/α-CD particles

The enzyme encapsulation efficiency of the hollow nanospheres was investigated with a GOX loading of 0.5 mg. Table 2 reveals that the encapsulation efficiency of GOX increased with increasing the concentration of CKGM-*g*-PEG. This maybe due to the fact that the number of hollow spheres formed increased as the concentration of polymer increased. The encapsulation efficiency was highest (67.0%) when the concentration of CKGM-*g*-PEG was highest at 0.5%.

3.5. Leakage of GOX from the CKGM-*g*-PEG/α-CD particles and the semi-permeability of the matrix

The main goal behind enzyme encapsulation is to entrap the protein in a semipermeable matrix, while allowing for penetration of substrate. Table 2 lists the GOX leakage data for different CKGM-*g*-PEG/α-CD systems after 48 h at 4 °C. It can be seen that the leakage efficiency was low for all of the samples. The lowest value of leakage efficiency was only 2%, which can be considered negligible loss. Furthermore, the comparative activity of encapsulated and free GOX indicated that glucose passes freely through the membrane of CKGM-*g*-PEG/α-CD nanospheres and be oxidized by the encapsulated enzyme.

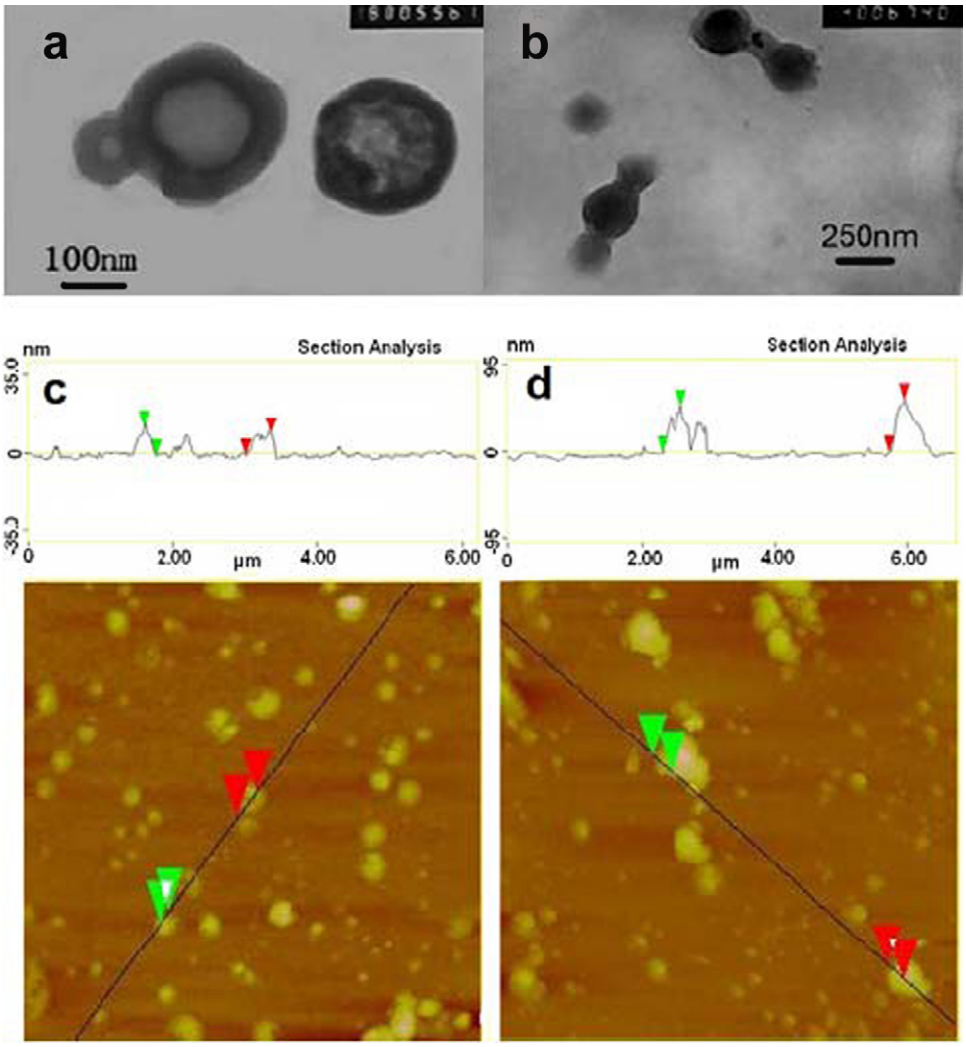

Fig. 4. TEM micrograph of (a) CKGM-g-PEG/α-CD (0.2% CP200/6% α-CD) hollow particles (b) CKGM-g-PEG/α-CD (0.2% CP200/6% α-CD) particles with GOX. Cross section analysis and height image of the AFM morphologies of (c) the hollow spheres and (d) the enzyme loaded spheres.

3.6. The activities of the encapsulated and free GOX

3.6.1. Effect of the reaction temperature on the activities of the encapsulated and free GOX

The activities of the free and encapsulated GOX were measured by maintaining the reaction medium in a thermal bath at a constant temperature from 25 to 45 °C. As shown in Fig. 5a, the optimal temperature for attainment the highest activities of both free and encapsulated GOX was 30 °C. However, the relative activity of the encapsulated enzyme was higher than that of the free enzyme from 25 °C to 45 °C, presumably owing to the improved thermal stability of the encapsulated enzyme in such microenvironments.

Table 2
The mean diameter, encapsulation efficiency, leakage efficiency of the CKGM-g-PEG/α-CD particles.

Concentrations of CP200 (w/v, %)	Mean diameter[a] (nm)	Encapsulation efficiency (%)	Leakage efficiency (%)
0.1	340 ± 35	52.73	12.35
0.2	402 ± 50	55.35	7.29
0.3	386 ± 39	66.22	2.04
0.4	487 ± 48	62.67	10.33
0.5	457 ± 36	67.09	5.30

[a] The nanospheres were formed by CP200 and 6.0% α-CD.

3.6.2. The thermostability of the encapsulated and free GOX

Proteins are readily denaturated by heat which includes irreversible lose of enzymatic activity. To determine the effect of encapsulation on enzyme thermostability, free and encapsulated GOX were incubated at a fixed temperature of 47 °C and monitored for relative activities over time. As shown in Fig. 5b a significant decrease in activity for both enzyme systems occurred with the increasing incubation time, yet the stability profiles of the free and encapsulated GOX were clearly different. After 150 min thermoincubation, the relative activity of the encapsulated enzyme remained nearly 90%, while that of the free enzyme was well below 70%. This observed increase in thermostability after encapsulation is probably due to nanosphere reducing the mobility of the enzyme and effectively shielding it from thermoeffects of the environment (Taqieddin & Amiji, 2004).

3.6.3. Effect of pH on the activities of the encapsulated and free GOX

Since the microenvironments of the encapsulated matrix may be altered by pH, we measured enzymatic activity of the free and encapsulated GOX as a function of changing pH conditions. The reaction medium pH value was adjusted in the range from 3.0 to 9.0. As shown in Fig. 5c, the free GOX showed maximum activity at pH 5.0, while the optimal pH of the encapsulated enzyme occurred

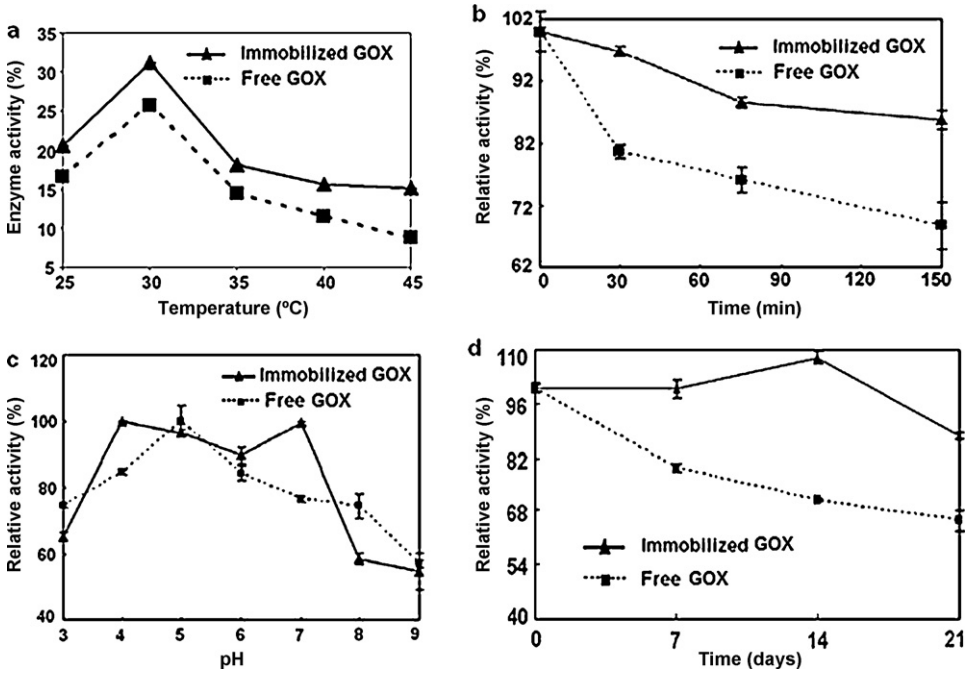

Fig. 5. (a) Temperature effect on activities of immobilized and free GOX. Immobilized and free GOX were stored in 0.2 M pH 6.5 acetate buffer. (b) Thermostability of the immobilized and free GOX at 47 °C. The immobilized and free GOX were stored in 0.2 M pH 6.5 acetate buffer. (c) Effect of the reaction pH on the activities of the immobilized and free GOX. (d) Storage stabilities of the immobilized and free GOX. The immobilized and free GOX were stored in 0.2 M acetate buffer (pH 6.5) at 4 °C.

over a broader range i.e. pH 4.0–7.0. Encapsulation is expected to alter the optimum pH of the enzyme (Vikartovská et al., 2007), as we found in agreement the pH-activity profile of encapsulated GOX increased slightly toward the alkaline side. These results indicate that encapsulation of GOX in CKGM-*g*-PEG/α-CD nanospheres stabilizes its enzymatic activity over a broader pH range compared with the free enzyme.

3.6.4. *Storage stability of the encapsulated and free GOX*

The long-term stability of encapsulated enzymes is an important criterion for most practical applications. Storage stability of encapsulated and free GOX at 4 °C was therefore investigated with the corresponding results illustrated in Fig. 5d. After one week, encapsulated GOX exhibited almost full activity, while free GOX retained only 75% activity. Even after 21 days, the encapsulated GOX exhibited nearly 90% of its initial activity, as activity of the free GOX was reduced to only 68%. These results confirm that our CKGM-*g*-PEG/α-CD encapsulation technique significantly improved the GOX storage stability.

3.7. *Biocompatibility of the CKGM-g-PEG/α-CD particles*

MTT is a pale yellow reagent, which is reduced by enzymes to a dark blue formazan product when incubated with viable cells. Therefore, the conversion of MTT into formazan can be used as a measure of cellular metabolism and viability. Fig. 6 shows effects of CKGM-*g*-PEG/α-CD concentrations on relative L929 cell growth after 24 h. Cell viability remained near 100% at concentrations ranging from 0.125 to 1.0 mg/mL after 24 h. From results of these MTT assays, it appears that CKGM-*g*-PEG/α-CD nanospheres are sufficiently biocompatible for use as a biological matrix but more comprehensive studies in specific organisms may be still needed.

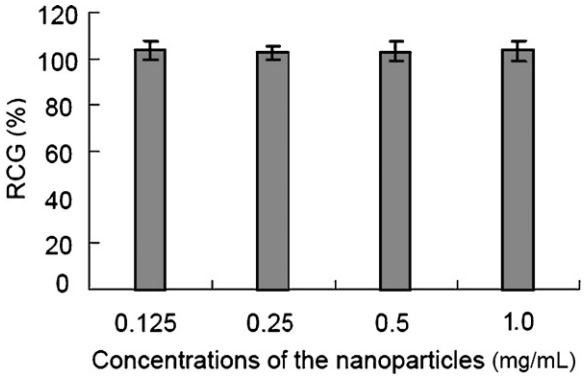

Fig. 6. Relative cell growth of L929 cells against the hollow nanospheres after cultured for 24 h with different nanosphere concentrations. Cell viability was estimated by MTT assay and expressed as percent of the blank control cells containing cell culture medium without nanospheres.

4. Conclusion

In summary, self-assembled CKGM-*g*-PEG/α-CD hollow nanospheres were prepared as a novel biocompatible matrix for glucose oxidase encapsulation. The strategy for fabrication was based on the self-assembly of rod–coil complexes, in which rod-like segments were formed by cyclodextrin inclusion. These hollow nanospheres showed semi-permeability and the encapsulated GOX exhibited significantly higher stability and sustained enzyme activity over a greater range of pH and temperature environments when compared with the free enzyme. In addition to these relevant attributes, the biocompatibility of CKGM-*g*-PEG/α-CD hollow nanospheres described in this study indicate that they are suitable for certain applications in enzyme encapsulation, bioreactors, or as biosensor devices.

Acknowledgements

This work was founded by the National Natural Science Foundation of China (NSFC Grant Nos. 21074138, 51073107 and 50703025) and the Opening Project of State Key Laboratory of Polymer Materials Engineering (Sichuan University) (Grant No. KF201003).

Appendix A. Supplementary data

Supplementary data associated with this article can be found, in the online version, at doi:10.1016/j.carbpol.2011.04.017.

References

Bradford, M. M. (1976). A rapid and sensitive method for the quantitation of microgram quantities of protein utilizing the principle of protein–dye binding. *Analytical Biochemistry*, *72*, 248–254.

Caroso, F., Caroso, R. A., & Möhwald, H. (1998). Nanoengineering of inorganic and hybrid hollow spheres by colloidal templating. *Science*, *282*, 1111–1114.

Ceccato, M., Nostro, P. L., & Baglioni, P. (1997). α-Cyclodextrin/polyethylene glycol polyrotaxane: A study of the threading process. *Langmuir*, *13*, 2436–2439.

Chen, D. Y., & Jiang, M. (2005). Strategies for constructing polymeric micelles and hollow spheres in solution via specific intermolecular interactions. *Accounts of Chemical Research*, *38*, 494–502.

Chen, H. L., Cheng, H. C., Liu, Y. J., Liu, S. Y., & Wu, W. T. (2006). Konjac acts as a natural laxative by increasing stool bulk and improving colonic ecology in healthy adults. *Nutrition*, *22*, 1112–1119.

Dai, G. L., Li, J. R., & Jiang, L. (1998). Assembly and folding of glucose oxidase at the water–air surface. *Annals of the New York Academy of Sciences*, *864*, 393–398.

Du, J., & O'Reilly, R. K. (2009). Advances and challenges in smart and functional polymer vesicles. *Soft Matter*, *5*, 3544–3561.

Du, J., Sun, R., Zhang, S., Govender, T., Zhang, L. F., Xiong, C. D., et al. (2004). Novel polyelectrolyte carboxymethyl konjac glucomannan–chitosan nanoparticles for drug delivery. *Macromolecular Rapid Communications*, *25*, 954–958.

Duan, H. W., Chen, D. Y., Jiang, M., Gan, W. J., Li, S. J., Wang, M., et al. (2001). Self-assembly of unlike homopolymers into hollow spheres in nonselective solvent. *Journal of the American Chemical Society*, *123*, 12097–12098.

Duan, H. W., Kuang, M., Wang, J., Chen, D. Y., & Jiang, M. (2004). Self-assembly of rigid and coil polymers into hollow spheres in their common solvent. *Journal of Physical Chemistry B*, *108*, 550–555.

Ha, W., Meng, X. W., Li, Q., Fan, M. M., Peng, S. L., Ding, L. S., et al. (2010). Self-assembly hollow nanosphere for enzyme encapsulation. *Soft Matter*, *6*, 1405–1408.

Harada, A., & Kamachi, M. (1990). Complex formation between poly(ethy1ene glycol) and α-cyclodextrin. *Macromolecules*, *23*, 2821–2823.

Harada, A., Li, J., & Kamachi, M. (1993). Preparation and properties of inclusion complexes of poly(ethy1ene glycol) with α-cyclodextrin. *Macromolecules*, *26*, 5698–5703.

Jenekhe, S. A., & Chen, X. L. (1998). Self-assembled aggregates of rod–coil block copolymers and their solubilization and encapsulation of fullerenes. *Science*, *279*, 1903–1907.

Jenekhe, S. A., & Chen, X. L. (1999). Self-assembly of ordered microporous materials from rod–coil block copolymers. *Science*, *283*, 372–375.

Kabayashi, S., Tsujihata, S., Hibi, N., & Tsukamoto, Y. (2002). Preparation and rheological characterization of carboxymethyl konjac gucomannan. *Food Hydrocolloids*, *16*, 289–294.

Li, B., Xia, J., Wang, Y., & Xie, B. J. (2005). Grain-size effect on the structure and antiobesity activity of konjac flour. *Journal of Agriculture and Food Chemistry*, *53*, 7404–7407.

Li, J. R., Du, Y. K., Boullanger, P., & Jiang, L. (1999). The folding and enzymatic activity of glucose oxidase in the glycolipid matrixes of different charges. *Thin Solid Films*, *352*, 213–217.

Lin, Y. H., Lu, F., Tu, Y., & Ren, Z. F. (2004). Glucose biosensors based on carbon nanotube nanoelectrode ensembles. *Nano Letters*, *4*, 191–195.

Luo, J. T., Xiao, K., Li, Y. P., Lee, J. S., Shi, L. F., Tan, Y. H., et al. (2010). Well-defined, size-tunable, multifunctional micelles for efficient paclitaxel delivery for cancer treatment. *Bioconjugate Chemistry*, *21*, 1216–1224.

Meng, X. W., Qin, J., Liu, Y., Fan, M. M., Li, B. J., Zhang, S., et al. (2010). Degradable hollow spheres based on self-assembly inclusion. *Chemical Communications*, *46*, 643–645.

Nakano, M., Takikawa, K., & Arita, T. (1979). Release characteristics of dibucaine dispersed in Konjac gels. *Journal of Biomedical Materials Research*, *13*, 811–819.

Napoli, A., Boerakker, M. J., Tirelli, N., Nolte, R. J. M., Sommerdijk, N. A. J. M., & Hubbell, J. A. (2004). Glucose-oxidase based self-destructing polymeric vesicles. *Langmuir*, *20*, 3488–3491.

Pandey, P., Singh, S. P., Arya, S. K., Gupta, V., Datta, M., Singh, S., et al. (2007). Application of thiolated gold nanoparticles for the enhancement of glucose oxidase activity. *Langmuir*, *23*, 3333–3337.

Qiu, Y., & Park, K. (2001). Environment-sensitive hydrogels for drug delivery. *Advanced Drug Delivery Reviews*, *53*, 321–339.

Smith, R. J. (1967). *Starch: Chemistry and technology*. New York: Academic Press.

Taqieddin, E., & Amiji, M. (2004). Enzyme immobilization in novel alginate–chitosan core–shell microcapsules. *Biomaterials*, *25*, 1937–1945.

Taylor, R. (1991). *Protein encapsulation: Fundamentals and applications*. New York: Marcel Dekker Inc.

Trau, D., & Renneberg, R. (2003). Encapsulation of glucose oxidase microparticles within a nanoscale layer-by-layer film: Immobilization and biosensor applications. *Biosensors and Bioelectronics*, *18*, 1491–1499.

Vikartovská, A., Bučko, M., Mislovičová, D., Pätoprstý, V., Lacík, I., & Gemeiner, P. (2007). Improvement of the stability of glucose oxidase *via* encapsulation in sodium alginate–cellulose sulfate-poly(methylene-*co*-guanidine) capsules. *Enzyme and Microbial Technology*, *41*, 748–755.

Wang, K., & He, Z. M. (2002). Alginate-konjac glucomannan chitosan beads as controlled release matrix. *International Journal of Pharmaceutics*, *244*, 117–126.

Wang, R., Xia, B., Li, B. J., Peng, S. L., Ding, L. S., & Zhang, S. (2008). Semi-permeable nanocapsules of konjac glucomannan–chitosan for enzyme immobilization. *International Journal of Pharmaceutics*, *364*, 102–107.

Wu, H. Y., & Chen, Y. (2008). Study on cytotoxicity of carboxymethyl glucomannan to L929 mouse fibroblasts in vitro. *Food Science (Chinese)*, *29*, 416–419.

Xia, B., Ha, W., Meng, X. W., Govender, T., Peng, S. L., Ding, L. S., et al. (2010). Preparation and characterization of a poly(ethylene glycol) grafted carboxymethyl konjac glucomannan copolymer. *Carbohydrate Polymers*, *79*, 648–654.

Xu, X., & Asher, S. A. (2004). Synthesis and utilization of monodisperse hollow polymeric particles in photonic crystals. *Journal of the American Chemical Society*, *126*, 7940–7945.

Zhou, J. Q., Chen, S. H., & Wang, J. W. (2008). A simple and convenient method to determine the activity of glucose oxidase. *Experimental Technology and Management (Chinese)*, *12*, 58–60.

Zhu, H. G., Srivastava, R., Brown, J. Q., & McShane, M. J. (2005). Combined physical and chemical immobilization of glucose oxidase in alginate microspheres improves stability of encapsulation and activity. *Bioconjugate Chemistry*, *16*, 1451–1458.